Photofunctional Nanomodulators for Bioexcitation

Eijiro Miyako,* Julie Russier, Matteo Mauro, Cristina Cebrian, Hiromu Yawo, Cécilia Ménard-Moyon, James A. Hutchison, Masako Yudasaka, Sumio Iijima, Luisa De Cola, and Alberto Bianco*

Abstract: A single organism comprises diverse types of cells. To acquire a detailed understanding of the biological functions of each cell, comprehensive control and analysis of homeostatic processes at the single-cell level are required. In this study, we develop a new type of light-driven nanomodulator comprising dye-functionalized carbon nanohorns (CNHs) that generate heat and reactive oxygen species under biologically transparent near-infrared (NIR) laser irradiation. By exploiting the physicochemical properties of the nanohorns, cellular calcium ion flux and membrane currents were successfully controlled at the single-cell level. In addition, the nanomodulator allows a remote bioexcitation of tissues during NIR laser exposure making this system a powerful tool for single-cell analyses and innovative cell therapies.

Non-invasive remote control technologies designed to manipulate cellular functions[1] are useful for the comprehensive and quantitative analysis of molecular and cellular processes. Most studies on single cells are performed in vitro using microfluidic devices.[2] However, this approach is limited to the observation of cell behavior in an "artificial" biological environment. Real-time analysis of functional biomolecules in the multicell context of a whole living body or organ may provide breakthroughs in the evaluation of molecular events at the single-cell level.

Optical regulation of cellular functions and optogenetic control of receptors and channel proteins on the surface of a cell have received particular attention because these approaches can aid in the development of next-generation tools for single-cell analyses[3] as well as of advanced cell therapies such as deep brain stimulation[4] and diabetes treatment.[5] The techniques currently used to control cellular functions rely on ultraviolet (UV),[5] short-wavelength visible (Vis),[6] and infrared (IR)[7] light sources. However, light at these wavelengths does not efficiently penetrate biological tissues. In contrast, near-infrared (NIR) light penetrates deeply into tissues because biological systems are transparent within this spectral window.[8] Among the different types of nanomaterials that can be excited in the NIR region, carbon-based nanomaterials, including carbon nanotubes (CNTs) and CNHs hold a lot of promises.[9–14] In particular, CNTs and CNHs exhibit extraordinary photothermal energy conversion efficiency and high absorption cross-sections in the NIR region.[9,10]

In this study, we demonstrate: 1) the ability of dye-functionalized CNHs to absorb NIR irradiation and to generate high levels of thermal energy and reactive oxygen species (ROS); 2) an increase of the photothermal generation of CNHs mediated by photoinduced processes triggered by the dye; 3) the biocompatibility of functionalized CNHs and their utility in NIR bioimaging with low background emission; and 4) the optical stimulation of diverse individual targeted cells and tissue functions by the functionalized CNHs. These carbon-based structures thus have great potential for the manipulation of single-cell behavior in vivo, and for the development of innovative cell therapies. Finally, our designed photoactive nanomodulators will also enable the analysis of "live" and "real" molecular events occurring in a living body for a comprehensive recovery of biomolecular information.

To develop an effective and safe NIR-laser-driven cellular stimulation system, we have functionalized CNHs with small organic molecules. We have selected CNHs because of their relatively high biocompatibility both in vitro and in vivo in comparison to more investigated CNTs.[10,13] Indeed, the CNTs often contain metal catalyst impurities that may remain after their synthesis.[15] To build the nanomodulator, CNHs were coupled to the fluorescent IRDye800CW through a 2,2′-(ethylenedioxy)bis(ethylamine) spacer (Figure 1). First, we optimized the reaction preparing several amino-functionalized CNHs (NH₂-CNHs) (Table S1). The maximum amino loading (ca. $320\ \mu mol\,g^{-1}$, 4.7 wt% as assessed by the Kaiser

[*] Dr. E. Miyako, Dr. M. Yudasaka, Prof. S. Iijima
Nanotube Research Center (NTRC), National Institute of Advanced Industrial Science and Technology (AIST)
Central 5, 1-1-1 Higashi, Tsukuba 305-8565 (Japan)
E-mail: e-miyako@aist.go.jp

Dr. J. Russier, Dr. C. Ménard-Moyon, Dr. A. Bianco
CNRS, Institut de Biologie Moléculaire et Cellulaire
Laboratoire d'Immunopathologie et Chimie Thérapeutique
15 Rue René Descartes, 67084 Strasbourg (France)
E-mail: a.bianco@ibmc-cnrs.unistra.fr

Dr. M. Mauro, Dr. C. Cebrian, Prof. L. De Cola
Laboratoire de Chimie et des Biomatériaux Supramoléculaires
Institut de Science et d'Ingénierie Supramoléculaires (ISIS)
Université de Strasbourg and CNRS
8 allée Gaspard Monge, 67083 Strasbourg (France)

Prof. H. Yawo
Department of Developmental Biology and Neuroscience
Tohoku University, Graduate School of Life Sciences
Sendai 980-8577 (Japan)

Dr. J. A. Hutchison
Laboratoire des Nanostructures
Institut de Science et d'Ingénierie Supramoléculaires (ISIS)
Université de Strasbourg and CNRS
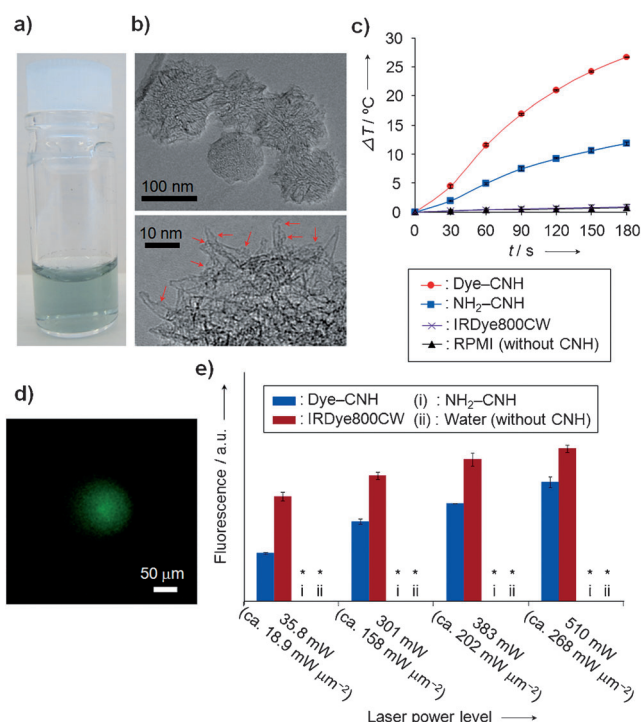8 allée Gaspard Monge, 67083 Strasbourg (France)
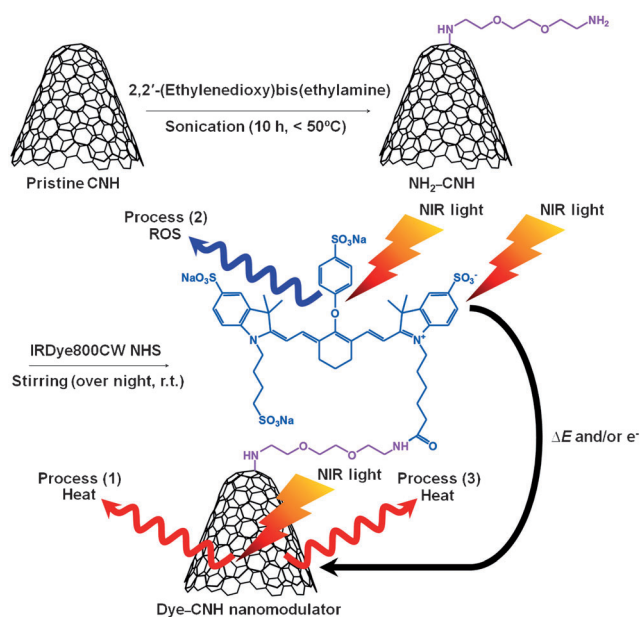
Figure 1. Illustration of the photofunctional nanomodulator. (1) Thermogenesis through photothermal conversion by CNHs. (2) ROS generation by IRDye800CW. (3) Thermogenesis through energy and/or electron transfer from IRDye800CW to CNH.

Figure 2. Characterization of the nanomodulators. a) Nanomodulator suspension (25 $\mu g\,mL^{-1}$). b) HRTEM images. Red arrows indicate the presence of organic material derived from 2,2′-(ethylenedioxy)bis(ethyl-amine) and IRDye800CW. c) Temperature changes of CNHs irradiated at 800 nm with a pulsed laser of 1.9 W ($\approx 264\,mW\,mm^{-2}$) for 3 min. Sample concentrations: dye-CNH = 100 $\mu g\,mL^{-1}$, NH$_2$-CNH = 75 $\mu g\,mL^{-1}$, IRDye800CW = 25 $\mu g\,mL^{-1}$. d) Real-time observation of ROS generated by photoinduced dye-CNH. e) Variation of fluorescence intensity of ROS using various CNHs irradiated with a NIR laser. Sample concentrations: dye-CNH = 12.5 $\mu g\,mL^{-1}$, NH$_2$-CNH = 9.4 $\mu g\,mL^{-1}$, IRDye800CW = 3.1 $\mu g\,mL^{-1}$. * No significant change in fluorescence intensity.

test) was achieved using a simple sonication method (Table S1, entry 3; Figure S1). NH$_2$-CNHs were directly conjugated to IRDye800CW activated as *N*-hydroxysuccinimide (NHS) ester (yield $\approx 63\%$). The mass loading of the dye on the CNHs was about 25 wt% as assessed by the Kaiser test. This dye was chosen as it can generate ROS through NIR light absorption and successive electron/energy evolution to activate oxygen species [for example, singlet oxygen ($^1O_2$)].[16–18] On the other hand, the CNHs absorb NIR light and generate heat by photothermal conversion. In this study we found that the heat generation by CNHs was enhanced by the good absorbing properties of the dye molecules: upon excitation of the dye, a part of the excitation energy is likely transferred to the lower energy levels of CNHs and relaxed by thermal conversion. Thus, the dye-labeled CNHs generate both heat and ROS as schematically depicted in Figure 1. Opposite to pristine CNHs, that are hydrophobic and insoluble in aqueous solvents,[10,13] CNHs functionalized with the dye (dye-CNH) were stable in water for up to 24 h (Figures 2a and S2) and displayed low cytotoxicity (Figure S3). The structure of the dye-CNHs was observed by high-resolution transmission electron microscopy (HRTEM) (Figures 2b and S4). The structures of individual nanohorns (i.e., conical tips) were preserved after functionalization.

NIR laser irradiation at 800 nm increased the temperature of the cell culture medium (RPMI) suspension of the dye-CNHs over time (Figure 2c). This temperature rise depended on the employed laser power (Figure S5a). The maximum temperature difference (ΔT_{max}) was approximately 27°C, whereas ΔT_{max} of the NH$_2$-CNH suspension was only about 12°C. No temperature changes were observed for the irradiated suspensions without CNHs or with only IRDye800CW (Figure 2c). From these data, we can conclude

that the dye has no intrinsic photothermal effect, even though it can enhance the exothermic power of CNHs. The proposed mechanism for ΔT enhancement is that the dye harvests the light energy and transfers it to CNHs by photoinduced processes (energy and/or electron transfer; Figure S6).[14,16] A similar effect could be observed in case of the aggregation of dyes forming clusters that could deactivate non-radiatively leading to an increase of heat.[19] However, this explanation is unlikely in our case, because due to the charged sulfonate groups the species are well solvated. Furthermore, we did not observe any change in the absorption profile, supporting a perturbation of the levels of the monomeric species or the formation of any type of aggregates.

Functional fluorophores are fundamental components in photodynamic therapy because they can generate ROS.[17] It is also known that ROS regulate ion channel activities that play a central step in many ROS-mediated processes, such as stress, hormone signaling, and immunological responses.[20] Therefore, we decided to study the capacity of dye-CNH nanomodulators to generate ROS by NIR laser irradiation for controlling cellular activity. ROS were detected by using 2′,7′-dichlorodihydrofluorescein diacetate (H2DCF-DA).[21] We observed a bright green fluorescence during 808 nm laser

irradiation (Figure 2 d and supporting video 1). Figure 2 e shows the fluorescence profiles at four different laser powers. The fluorescence intensities of the green spots significantly increased as a function of NIR laser power using both dye-CNHs and IRDye800CW. The average fluorescence intensity of the ROS probe was lower for the cells treated with dye-CNHs in comparison to IRDye800CW, for each applied power. We carefully adjusted the concentration of free dye and the dye attached to the CNHs to the same value. The decrease of the efficiency in the generation of ROS, in the case of IRDye800CW linked to the CNH, is most likely due to a competitive pathway which involves a photoinduced process,[22] through either an electron or an energy transfer, from the dye onto the carbon material (Figure 1, process 3).[14, 16] No ROS was generated upon NIR laser irradiation of NH_2-CNH or just water (Figure 2 e). This finding suggests that the dye-CNHs irradiated with NIR light are able to produce both heat and ROS (Figure 1). In a control experiment, green fluorescence of the ROS probe was totally absent when aqueous solutions of dye-CNH or IRDye800CW were excited by NIR laser in the presence of ROS inhibitor N-acetyl-L-cysteine (NAC) (data not shown).[23]

Calcium influx is one of the most important processes in the physiology and biochemistry of organisms and cells.[1] Indeed, it plays a pivotal role in a variety of biomolecular events (e.g., neurotransmitter release from neurons, muscular contraction, and enzymatic reactions). One of the main objectives of this study was to demonstrate the remote control of inter/intracellular Ca^{2+} flux by photoinduced dye-CNHs. To accomplish this challenging goal, we incubated the dye-CNH nanomodulators with cells expressing temperature-activated transient receptor potential ion channels (thermo-TRPs) and calcium ion channels (e.g., the inositol triphosphate (IP_3) receptor), and then irradiated the cells using a NIR laser. The increase of local temperature and the generation of high level of ROS opened thermo-TRPs and ion channels, causing an influx and/or release of Ca^{2+} from intracellular compartments (Figure 3 a). To determine whether the nanomodulator-generated local heat and ROS were sufficient to regulate the activity of these channels, we observed the intracellular calcium flux using Fluo-8.[24] For this purpose, we used ND7/23 hybrid cells derived from mouse neuroblastoma and rat neuron cells, mouse leukemic monocyte-derived macrophages (RAW264.7), and human cervical cancer cells (HeLa). Only ND7/23 cells overexpress thermo-TRPs.[25] When ND7/23 cells harboring the internalized dye-CNH nanomodulators were irradiated at 808 nm (laser power: 204 mW (ca. 104 µW µm^{-2}); laser spot diameter about 50 µm; Figure S7 a), we immediately observed a bright green fluorescence caused by calcium influx (Figure 3 b and supporting video 2). A similar enhancement of the calcium probe fluorescence intensity was measured in RAW264.7 and to a lower extent in HeLa cells (Figure S8). However, the difference of the fluorescence intensity between RAW264.7 and ND7/23 was not statistically significant. The higher internalization of dye-CNHs by phagocytic RAW264.7 may contribute to their large Ca^{2+} influx and compensate their lower TRP expression in comparison to ND7/23. Intracellular localization of dye-CNHs in the three types of cells was
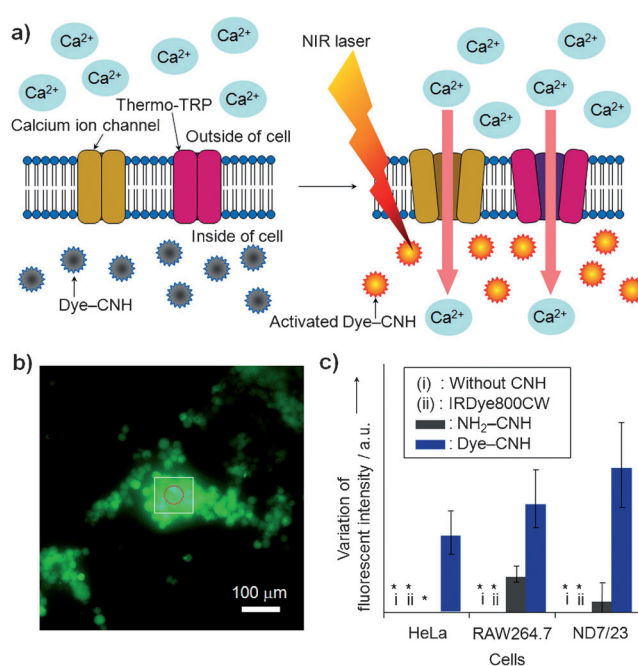
Figure 3. Cellular stimulation by the nanomodulators. a) Illustration of the control of cellular activity by photoinduced nanomodulators. b) Calcium imaging in ND7/23 cells detected by fluorescence emission of Fluo-8 by laser-induced dye-CNH [204 mW (ca. 104 µW µm^{-2})]. The white square shows the site of fluorescence analysis. The red circle indicates the irradiated site. c) Analysis of fluorescence emission by irradiated cells that have internalized dye-CNHs. * No significant difference in fluorescence intensity.

confirmed using NIR fluorescence microscopy (Figures S7 d and S10). A reduction of the fluorescence derived from Ca^{2+} influx in RAW264.7 and ND7/23 cells was also observed using NAC (Figure S9).

In contrast, NH_2-CNH induced only a slight increase of calcium probe fluorescence intensity in irradiated RAW264.7 and ND7/23 cells. No significant changes in the fluorescence intensity were measured in the absence of CNHs or in the presence of IRDye800CW alone, indicating that dye-functionalized CNHs are able to stimulate diverse types of cells (Figure 3 c). Moreover, the viability of the cells that have internalized the nanomodulators was not affected under laser irradiation using the laser power necessary to induce Ca^{2+} influx [≤ 204 mW (ca. 104 µW µm^{-2})] (Table S2 and supporting video 3). The maximum variation in fluorescence intensity occurred in irradiated ND7/23 cells. This is due to the fact that only ND7/23 cells overexpress thermo-TRPs[25] and incorporate Ca^{2+} ions more efficiently, triggered by the photothermal property of the nanomodulators. Using the cell patch clamp technique,[26] we also analyzed the membrane current of primary cultures of rat dorsal root ganglion (DRG) cells that express thermo-TRPs (Figure S7 b,c). We measured a significant change in the membrane current of DRGs with increased laser powers. Although previous studies have shown that NIR excitation modulates biological functions, the exact mechanism of these effects is still unknown. Cellular stimulation induced by NIR irradiation is accompanied by rapid increases in temperature,[7] which may stimulate cells by affecting ion

channel gating, activating intracellular second messengers, forming membrane pores, triggering thermosensitive ion channels, or increasing membrane conductance. There is no direct evidence supporting these mechanisms. Nonetheless, the nanomodulator described here is an effective biostimulator under a continuous-wave low-power laser irradiation.[7,26,27]

To explore the future potential of our nanomodulators in a living model, we used laser-triggered remote bioexcitation of a *Xenopus laevis* paw (Figure 4a and supporting video 4).
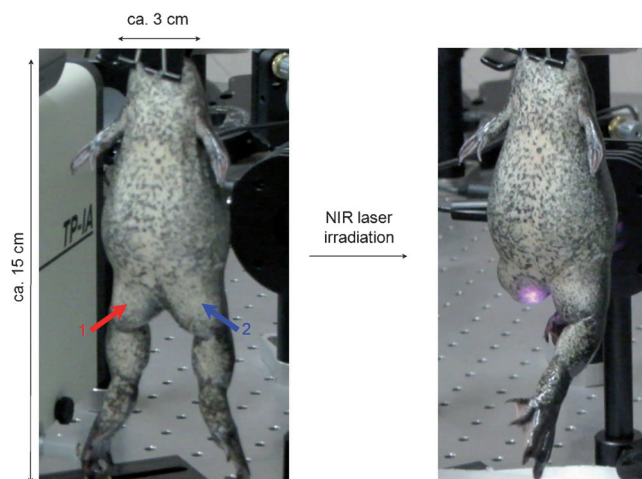
Figure 4. Laser-driven remote stimulation of a frog (*X. laevis*) paw before (left) and after laser irradiation (right). Red and blue arrows show the location where the dye-CNH (1) and Ringer solution (2) were injected. Sample concentrations: dye-CNH = 300 µg mL^{-1}, NH$_2$-CNH = 225 µg mL^{-1}, IRDye800CW = 75 µg mL^{-1}.

Dye-CNHs were injected under the thigh of the euthanized frog. Immediately after irradiation started [at 800 nm, 2.1 W (ca. 292 mW mm^{-2})], the paw twitched. The same movement was absent when only NH$_2$-CNH, IRDyeCW800, or Ringer solution without CNHs were injected. *X. laevis* have nerves that express thermo-TRPs and a variety of other channel proteins.[28] NIR light can penetrate into the tissue up to 10 cm,[8] allowing dye-CNH nanomodulators to be noninvasively excited within a significant area of the thigh. We also observed the relatively high temperature increase of the paw surface when the dye-CNH nanomodulator was administered (Figure S11). These results indicate that the dye-CNHs have the possibility to mediate the stimulation of cells in *X. laevis* tissues, resulting in significant bioexcitation.

In this study, we describe the design and applications of a photofunctional nanomodulator. CNHs were chemically modified with a short hydrophilic spacer and a NIR fluorophore and the molecular interface of the three moieties allowed generating heat and ROS when irradiated using an NIR laser. Intercellular Ca^{2+} flux and membrane currents could be optically controlled at the single-cell level using this nanomodulator. This is the first demonstration of remote control of cellular activities in vitro and in living species using a new type of nanomodulator that exploits the powerful physicochemical properties of dye-functionalized nanocar-

bons. This study provides a beneficial technology with potential applications in various areas of biology, including comprehensive analysis of signaling at the single-cell level, development of unique cell therapies and tissue engineering, and creation of wireless photobionic devices.

[1] B. Alberts, D. Bray, K. Hopkin, A. Johnson, J. Lewis, M. Raff, K. Roberts, P. Walter, *Essential Cell Biology*, 3rd ed., Garland, New York, **2009**.
[2] C. Kasper, *Eng. Life Sci.* **2009**, *9*, 407.
[3] H. Yawo, T. Asano, S. Sakai, T. Ishizuka, *Dev. Growth Differ.* **2013**, *55*, 474–490.
[4] V. Gradinaru, M. Mogri, K. R. Thompson, J. M. Henderson, K. Deisseroth, *Science* **2009**, *324*, 354–359.
[5] H. Ye, M. D. E. Baba, R.-W. Peng, M. Fussenegger, *Science* **2011**, *332*, 1565–1568.
[6] G. Leitz, E. Fällman, S. Tuck, O. Axner, *Biophys. J.* **2002**, *82*, 2224–2231.
[7] M. G. Shapiro, K. Homma, S. Villarreal, C.-P. Richter, F. Bezanilla, *Nat. Commun.* **2011**, *3*, 736.
[8] R. Weissleder, *Nat. Biotechnol.* **2001**, *19*, 316–317.
[9] E. Miyako, K. Kono, E. Yuba, C. Hosokawa, H. Nagai, Y. Hagihara, *Nat. Commun.* **2012**, *3*, 1226.
[10] E. Miyako, T. Deguchi, Y. Nakajima, M. Yudasaka, Y. Hagihara, M. Horie, M. Shichiri, Y. Higuchi, F. Yamashita, M. Hashida, Y. Shigeri, Y. Yoshida, S. Iijima, *Proc. Natl. Acad. Sci. USA* **2012**, *109*, 7523–7528.
[11] K. Kostarelos, L. Lacerda, G. Pastorin, W. Wu, S. Wieckowski, J. Luangsivilay, S. Godefroy, D. Pantarotto, J. P. Briand, S. Muller, M. Prato, A. Bianco, *Nat. Nanotechnol.* **2007**, *2*, 108–113.
[12] S. Lacotte, A. García, M. Décossas, W. T. Al-Jamal, S. Li, K. Kostarelos, S. Muller, M. Prato, H. Dumortier, A. Bianco, *Adv. Mater.* **2008**, *20*, 2421–2426.
[13] M. Zhang, M. Yudasaka, K. Ajima, J. Miyawaki, S. Iijima, *ACS Nano* **2007**, *1*, 265–272.
[14] G. Pagona, G. E. Zervaki, A. S. D. Sandanayaka, O. Ito, G. Charalambidis, T. Hasobe, A. G. Coutsolelos, N. Tagmatarchis, *J. Phys. Chem. C* **2012**, *116*, 9439–9449.
[15] V. L. Colvin, *Nat. Biotechnol.* **2003**, *21*, 1166–1170.
[16] A. S. D. Sandanayaka, O. Ito, M. Zhang, K. Ajima, S. Iijima, M. Yudasaka, T. Murakami, K. Tsuchida, *Adv. Mater.* **2009**, *21*, 4366–4371.
[17] M. Mitsunaga, M. Ogawa, N. Kosaka, L. T. Rosenblum, P. L. Choyke, H. Kobayashi, *Nat. Med.* **2011**, *17*, 1685–1691.
[18] X. Peng, D. R. Draney, W. M. Volcheck, G. R. Bashford, D. T. Lamb, D. L. Grone, Y. Zhang, C. M. Johnson, *Proc. SPIE-Int. Soc. Opt. Eng.* **2006**, *6097*, 113–124.
[19] J. Yu, D. Javier, M. A. Yaseen, N. Nitin, R. Richards-Kortum, B. Anvari, M. S. Wong, *J. Am. Chem. Soc.* **2010**, *132*, 1929–1938.
[20] Y. Yan, C.-L. Wei, W.-R. Zhang, H.-P. Cheng, J. Liu, *Acta Pharmacol. Sin.* **2006**, *27*, 821–826.
[21] R. P. Rastogi, S. P. Singh, D. P. Häder, R. P. Sinha, *Biochem. Biophys. Res. Commun.* **2010**, *397*, 603–607.
[22] K. Mizuno, J. Ishii, H. Kishida, Y. Hayamizu, S. Yasuda, D. N. Futaba, M. Yumura, K. Hata, *Proc. Natl. Acad. Sci. USA* **2009**, *106*, 6044–6047.
[23] M. Halasi, M. Wang, T. S. Chavan, V. Gaponenko, N. Hay, A. L. Gartel, *Biochem. J.* **2013**, *454*, 201–208.

[24] S. Falk, J. C. Rekling, *Neurosci. Lett.* **2009**, *450*, 229–234.

[25] D. Wu, W. Huang, P. M. Richardson, J. V. Priestley, M. Liu, *J. Biol. Chem.* **2008**, *283*, 416–426.

[26] M. A. Gandini, A. Sandoval, R. Felix, *Cold Spring Harbor Protoc.* **2014**, 4.

[27] T. Bruegmann, D. Malan, M. Hesse, T. Beiert, C. J. Fuegemann, B. K. Fleischmann, P. Sasse, *Nat. Methods* **2010**, *7*, 897–900.

[28] M. Ohkita, S. Saito, T. Imagawa, K. Takahashi, M. Tominaga, T. Ohta, *J. Biol. Chem.* **2012**, *287*, 2388–2397.